A simplified procedure for semi-targeted lipidomic analysis of oxidized phosphatidylcholines induced by UVA irradiation

Florian Gruber,* Wolfgang Bicker,† Olga V. Oskolkova,§ Erwin Tschachler,*, and Valery N. Bochkov[1,§]**

Department of Dermatology,* Medical University of Vienna, Vienna, Austria; FTC-Forensic-Toxicological Laboratory Ltd.,† Vienna, Austria; Department of Vascular Biology and Thrombosis Research,§ Center for Physiology and Pharmacology, Medical University of Vienna, Vienna, Austria; and CE.R.I.E.S,** Neuilly sur Seine, France

Abstract Oxidized phospholipids (OxPLs) are increasingly recognized as signaling mediators that are not only markers of oxidative stress but are also "makers" of pathology relevant to disease pathogenesis. Understanding the biological role of individual molecular species of OxPLs requires the knowledge of their concentration kinetics in cells and tissues. In this work, we describe a straightforward "fingerprinting" procedure for analysis of a broad spectrum of molecular species generated by oxidation of the four most abundant species of polyunsaturated phosphatidylcholines (OxPCs). The approach is based on liquid-liquid extraction followed by reversed-phase HPLC coupled to electrospray ionization MS/MS. More than 500 peaks corresponding in retention properties to polar and oxidized PCs were detected within 8 min at 99 *m/z* precursor values using a single diagnostic product ion in extracts from human dermal fibroblasts. Two hundred seventeen of these peaks were fluence-dependently and statistically significantly increased upon exposure of cells to UVA irradiation, suggesting that these are genuine oxidized or oxidatively fragmented species. This method of semitargeted lipidomic analysis may serve as a simple first step for characterization of specific "signatures" of OxPCs produced by different types of oxidative stress in order to select the most informative peaks for identification of their molecular structure and biological role.—Gruber, F., W. Bicker, O. V. Oskolkova, E. Tschachler, and V. N. Bochkov. **A simplified procedure for semi-targeted lipidomic analysis of oxidized phosphatidylcholines induced by UVA irradiation. *J. Lipid Res.* 2012.** 53: **1232–1242.**

Supplementary key words oxidized phospholipids • lipidomics • dermal fibroblasts • ultraviolet A irradiation

The work was supported by grants from Österreichische Forschungsförderungsgesellschaft (project 815445 to V.N.B.) and Fonds zur Förderung wissenschaftlicher Forschung (P20801-B11 to V.N.B. and P22267-B11 to O.V.O.).

Manuscript received 9 February 2012 and in revised form 1 March 2012.

Published, JLR Papers in Press, March 13, 2012
DOI 10.1194/jlr.D025270

Oxidized phospholipids (OxPLs) are generated by enzymatic or nonenzymatic oxidation of esterified PUFAs. Rapidly accumulating evidence suggests that OxPLs are pleiotropic lipid mediators potentially involved in the pathogenesis of a variety of disease states. Important biological activities of OxPLs include their proinflammatory action, proaggregant shift in endothelium and platelets, angiogenic effects, and modulation of innate and adaptive immune responses (1). Furthermore, the role of OxPLs as clinical biomarkers is being investigated. Available data suggest that circulating levels of OxPLs correlate with the presence and progression of atherosclerosis and predict cardiovascular events independently of traditional risk factors (2). Moreover, the relative contents of OxPLs per LDL particle may reflect the removal of cholesterol from tissues as a result of therapy with statins (3). Thus, OxPLs may become a novel class of diagnostic markers useful in predicting disease and monitoring efficiency of treatment.

Understanding the biological importance of OxPLs and their potential role as disease biomarkers requires obtaining precise information about concentrations of these compounds in cells and tissues, which is a challenging task because oxidation of PLs generates dozens of molecular

Abbreviations: BHT, butylated hydroxytoluene; CV, coefficient of variation; DNPC, 1,2-dinonanoyl-*sn*-glycero-3-phosphocholine; ESI, electrospray ionization; LLE, liquid-liquid extraction; OxPC, oxidized phosphatidylcholine; OxPL, oxidized phospholipid; PAzPC, 1-palmitoyl-2-azelaoyl-*sn*-glycero-3-phosphocholine; PAPC, 1-palmitoyl-2-arachidonoyl-*sn*-glycero-3-phosphocholine; PARP, poly ADP-ribose polymerase; PGPC, 1-palmitoyl-2-glutaroyl-*sn*-glycero-3-phosphocholine; PLPC, 1-palmitoyl-2-linoleoyl-*sn*-glycero-3-phosphocholine; PONPC, 1-palmitoyl-2-(9-oxo)nonanoyl-*sn*-glycero-3-phosphocholine; POVPC, 1-palmitoyl-2-(5-oxovaleroyl)-*sn*-glycero-3-phosphocholine; SAPC, 1-stearoyl-2-arachidonoyl-*sn*-glycero-3-phosphocholine; SLPC, 1-stearoyl-2-linoleoyl-*sn*-glycero-3-phosphocholine; SRM, selected reaction monitoring; UVA, ultraviolet A.

[1] To whom correspondence should be addressed.
e-mail: valery.bochkov@meduniwien.ac.at

species from each type of PUFA-containing unoxidized precursor (Supplementary Fig. I). The chemical diversity of oxidation products accumulating in vivo depends on many factors, including the relative impact of nonenzymatic versus enzymatic oxidation and variable tissue expression of enzymes oxidizing PLs directly (e.g., 15-LOX [4]) or enzymes oxidizing free fatty acids followed by esterification (5, 6), as well as enzymes reducing PL hydroperoxides (GPx4 [7] and peroxiredoxin 6 [8]).

Different molecular species of OxPLs often demonstrate nonidentical biological activities. For example, nonfragmented OxPLs induce barrier-protective effects in lung endothelium, whereas fragmented species are barrier disruptive (9). Similarly, exposure of dermal fibroblasts to UVA-generated, nonfragmented oxidized phosphatidylcholine (OxPCs) induced adaptive responses (10, 11), whereas production of fragmented species containing reactive carbonyl groups correlated to skin ageing (12) and pathologies of the skin that develop upon solar exposure, such as actinic elastosis (13).

In summary, because of the high complexity of the mechanisms of generation, degradation, and biological action of OxPLs, investigation of their role in specific (patho)physiological conditions requires monitoring a variety of oxidized species. Therefore, there is a need for procedures to analyze a broad spectrum of various OxPL classes.

Mass spectrometry is the most sensitive and universal method for quantification of OxPLs (14). Because of the tremendous excess of unoxidized lipids and the presence of isobaric peaks, analysis of individual OxPLs by mass spectrometry is only feasible after chromatographic separation of lipids, typically by reversed-phase HPLC. Previous publications described mass spectrometry-based methods for analysis of oxidized cardiolipin (15–17), phosphatidylserine (15, 16, 18), phosphatidylethanolamine (6, 19–22), and phosphatidylcholine (23–25 and references below). The results show that different PL classes have variable propensity for oxidation. For example, cardiolipin and phosphatidylserine were preferentially oxidized during apoptosis induced by radiation or hyperoxia, whereas the more abundant phosphatidylcholine and phosphatidylethanolamine remained unoxidized (15, 16). On the other hand, different types of pathology have variable effects on the oxidation of one class of PLs, as illustrated by different patterns of OxPLs observed in mouse models of Th1 and Th2 inflammation (26). Altogether, the available data suggest that oxidation of PLs is a common feature of pathology and that no universal marker of PL oxidation exists.

The data discussed above indicate a need for a comprehensive analytical technique capable of quantifying multiple oxidized species belonging to different PL classes. However, variation in charge of polar head groups and extreme diversity of oxidized species makes analysis of several classes of OxPLs within one analytical run impractical. Because of these limitations, our study focused on the detection of oxidized phosphatidylcholines (OxPCs), which represent an abundant class of OxPLs demonstrating a variety of biological activities but insufficiently characterized with respect to accumulation in cells and tissues. Previous studies described procedures for focused analysis of OxPCs containing fragmented ω-terminal (27), fragmented α,β-unsaturated (28, 29), fragmented terminal furan-containing (30), and nonfragmented linear (5, 24) and prostane ring-containing (31) residues. Here we show that a variety of full-length and fragmented OxPCs can be detected at 99 *m/z* precursor values using *m/z* 184 as a diagnostic fragment ion within one HPLC-electrospray ionization (ESI)-MS/MS run having a total run time of 20 min (including column re-equilibration). To prove the feasibility of peak identification, four molecular species were identified using spiking with commercial standards and fragmentation studies in negative ion mode. The method is sensitive, allowing detection of more than 500 peaks of oxidized and polar PCs upon injecting lipid extract from human dermal fibroblasts grown on a cell culture vessel surface of 1.6 cm^2. Our data show that the vast majority of these peaks, but not unoxidized PCs, were elevated upon oxidative stress induced by UVA irradiation. The method can be used as a simple starting procedure for a fingerprint-like characterization of patterns of PC oxidation under conditions of oxidative stress and disease.

MATERIALS AND METHODS

Materials

Human neonatal skin fibroblasts were obtained from Cascade Biologics (Portland, OR) and grown in DMEM (Gibco, Gaithersburg, MD) supplemented with 10% FCS and penicillin (100 U/ml)/streptomycin (100 μg/ml) to subconfluence.

Synthetic 1-palmitoyl-2-arachidonoyl-*sn*-glycero-3-phosphocholine (PAPC), 1-stearoyl-2-arachidonoyl-*sn*-glycero-3-phosphocholine (SAPC), 1-palmitoyl-2-linoleoyl-*sn*-glycero-3-phosphocholine (PLPC), 1-stearoyl-2-linoleoyl-*sn*-glycero-3-phosphocholine (SLPC), 1,2-dipalmitoyl-*sn*-glycero-3-phosphocholine (DPPC), 1-stearoyl-2-docosahexaenoyl-*sn*-glycero-3-phosphocholine (SDHPC), 1-palmitoyl-2-docosahexaenoyl-*sn*-glycero-3-phosphocholine (PDHPC), 1,2-dinonanoyl-*sn*-glycero-3-phosphocholine (DNPC), 1-palmitoyl-2-(5-oxovaleroyl)-*sn*-glycero-3-phosphocholine (POVPC), and 1-palmitoyl-2-glutaroyl-*sn*-glycero-3-phosphocholine (PGPC) were purchased from Avanti Polar Lipids (Alabaster, AL). 1-Palmitoyl-2-azelaoyl-*sn*-glycero-3-phosphocholine (PAzPC) and 1-palmitoyl-2-(9-oxo)nonanoyl-*sn*-glycero-3-phosphocholine (PONPC) were from Cayman Chemicals (Ann Arbor, MI). PAPC, PLPC, SAPC, and SLPC were oxidized by exposure of dry lipids to air for about 48 h until approximately 20% of the lipid remained intact and the rest was oxidized. Oxidized lipids were dissolved in chloroform, purged with argon. and stored at −70°C. Oxidation was monitored by thin-layer chromatography and electrospray ionization-mass spectrometry (27). Concentration of PLs was determined by phosphorus assay (32). Organic solvents were of analytical grade. Diethylenetriaminepentaacetic acid (DTPA) and butylated hydroxytoluene (BHT) were from Sigma-Aldrich (St. Louis, MO).

Irradiation of cells

UV irradiation was carried out as described previously (33). A Sellamed 3000 UVA-1 therapy lamp (Sellas, Ennepetal, Germany) filtered for the emission at 340–400 nm was used as a light source

at a distance of 20 cm. Cells in a 6-well plate containing 1 ml PBS per well were irradiated with 40 J/cm^2 (10 min) or 80 J/cm^2 (20 min) of UVA-1 on a cooling plate kept at 25°C. "Sham" cells were treated identically but without irradiation. For some experiments, the distance to the light source was increased according to the readings of a Waldmann UV meter in a way to obtain a half of irradiance level. At this longer distance, irradiation for 20 min produced a fluence of 40 J/cm^2 instead of the standard value of 80 J/cm^2.

Immediately after achieving the necessary UVA fluence, the cells were placed on ice, washed with PBS containing diethylenetriaminepentaacetic acid (2 mM) and BHT (0.01%), and scraped into 1 ml of methanol/acetic acid (3%)/BHT (0.01%). Identically treated samples were combined in pairs producing three samples for analysis, each containing cells from two 35 mm wells. The samples were purged with argon and stored at −70°C until purification by liquid-liquid extraction (LLE).

Liquid-liquid extraction

Combined samples from two identically treated wells in 2 ml methanol/acetic acid (3%)/BHT (0.01%) were supplemented with internal standard (1,2-dinonanoyl-*sn*-glycero-3-phosphocholine [DNPC], 20 ng per sample) and transferred to a 20-ml acid-washed glass tube, which was placed into a 2-l beaker containing ice and constantly purged with argon. The top of the tube was below the edges of the argon-filled beaker, thus protecting the sample from contact with air. The samples were washed with 4 ml hexane/BHT (0.01%) that was supplied from a dispenser filled with argon. The tube was additionally purged with argon, closed with a teflon-lined screw cap, and vortexed. The hexane layer was aspirated; due to significant difference in densities of the solvents, hexane could be removed almost completely. Any potential loss of methanolic phase was corrected by the presence of internal standard. After the third wash, 4 ml chloroform/BHT (0.01%) and 1.5 ml HCOOH (0.7 M) were added to the methanol phase, followed by vortexing. The lower organic phase was transferred to glass vials using a Pasteur pipette, dried under argon, and stored at −70°C until the mass spectrometry analysis.

The LLE procedure was as effective in separating lipid classes as the SPE-based technique that was used in our previous study (34). Complete removal of neutral lipids and fatty acids after three rounds of hexane extraction was confirmed by TLC on silica gel plates in chloroform/methanol/water = 100:50:10 and ethyl acetate/hexane = 80:20 (data not shown). Even after five washes, there was no visible loss in the amount of PCs, suggesting that the hexane/acidic methanol solvent pair produces selective and quantitative separation of PCs from neutral lipids and fatty acids.

To determine extraction yield, identical portions of lipid extract from fibroblasts corresponding to two wells in a 6-well dish were spiked with DNPC, POVPC, PGPC, PONPC, and PAzPC (50 ng each) before or after the LLE procedure. Lipid extract without added standards was used for determination of endogenous levels of these PCs; endogenous values were subtracted from the levels obtained for spiked samples. The yield was expressed as the ratio of analytes in samples spiked before the LLE to those spiked after. The procedure demonstrated reproducible yield (Supplementary Table I) acceptable for the purposes of relative quantification (i.e., comparison of treated and control samples). Some variation in extraction efficiencies between molecular species was observed. However, the difference is not critical because the method is intended for relative rather than absolute quantification. Removal of precipitated protein from methanol by centrifugation before hexane extraction did not significantly influence the yield, thus showing that acidic methanol effectively inhibited cellular phospholipases (Supplementary Table I).

HPLC-ESI-MS/MS

Samples purified by the LLE procedure were reconstituted in 85% aqueous methanol containing 5 mM ammonium formate and 0.1% formic acid. Aliquots (10 μL) were injected onto a core-shell-type C_{18} column (Kinetex 2.6 μm, 50 mm × 3.0 mm ID; Phenomenex, Torrance, CA) kept at 20°C and using a 1200 series HPLC system from Agilent Technologies (Waldbronn, Germany), which was coupled to a 4000 QTrap triple quadrupole linear ion trap hybrid mass spectrometer system equipped with a Turbo V electrospray ion source (Applied Biosystems, Foster City, CA). Elution was performed by a linear gradient of water (eluent A) and methanol (eluent B) both containing 5 mM ammonium formate and 0.1% formic acid. The time program was as follows: 0 min: 85% B; 2 min: 85% B; 3 min: 95% B; 11 min: 100% B; 16 min: 100% B; 16.1 min: 85% B; 20 min: 85% B. The flow rate of mobile phase was 0.4 ml/min from 0 to 3 min and was increased linearly to 0.6 ml/min until 11 min run time, kept constant at 0.6 ml/min until 19 min run time, and was reduced linearly to 0.4 ml/min until 20 min run time. Detection was carried out in positive ion mode by selected reaction monitoring (SRM) of 99 MS/MS transitions using a PC-specific product ion (*m/z* 184), which corresponds to the cleaved phosphocholine residue. The electrospray ionization voltage was set to 4500 V, and the temperature of the ion source was set to 550°C. Nitrogen was used as nebulizer, heater, and curtain gas with the pressure set at 50, 30, and 20 psi, respectively. SRM settings were as follows: declustering potential = 120, entrance potential = 10, collision energy = 53, cell exit potential = 14, and dwell time = 13 ms. Data acquisition and instrument control were performed with the Analyst software, version 1.5.1 from Applied Biosystems.

Although the current method is intended for relative quantification ("fingerprinting"), external calibration (i.e., using matrix-free standard solutions) was carried out for POVPC, PGPC, PONPC, and PAzPC to estimate linear range and sensitivity for these analytes. Concentrations of analytes were determined from calibration curves (1/x weighted linear regression) plotted as ratio of analyte peak area/DNPC peak area versus the amount of analyte on a column. Linear ranges, equations, and *r* values are summarized in Supplementary Table II.

Injection precision was determined by sequentially injecting (n = 6) the same sample of fibroblast lipid extract spiked with DNPC and fragmented OxPCs (i.e., POVPC, PGPC, PONPC, and PAzPC). The coefficients of variation (CVs) of peak areas of exogenously added OxPCs were 0.06, 0.05, 0.05, 0.04, and 0.03, respectively. The endogenous fragmented homologs SOVPC, SGPC, SONPC, and SAzPC demonstrated CVs of 0.06, 0.04, 0.04, and 0.1, respectively. Full-length endogenous OxPCs corresponding in retention time to PLPC-OH, PLPC-OOH, PAPC-OH, and PAPC-OOH were characterized by CVs of 0.03, 0.02, 0.02, and 0.04, respectively. Within-sequence precision of the sum of injection and extraction procedures in terms of CV of the internal standard was estimated by sequential injection of 40 different samples of fibroblasts that were spiked with DNPC before the extraction procedure. The CV for DNPC was 0.06. Altogether the data demonstrated the suitability of the analysis procedure for "fingerprinting" purposes.

Western blotting

Poly ADP-ribose polymerase (PARP) antibodies (Cell Signaling Technology, Danvers, MA) and GAPDH antibody (Abcam PLC, Cambridge, UK) were detected by anti-IgG conjugated with peroxidase and subsequent chemiluminescent imaging.

Statistics and visualization

Peaks significantly enhanced by treatment with 40 or 80 Joules per cm^2 were determined from the biological triplicates (each

containing lipids from two wells) using a *t*-test subsequently corrected with the Benjamini-Hochberg method (35) to achieve a false discovery rate of < 0.05. The mean values for each peak were clustered into three groups representing (*1*) the constant peaks, (*2*) peaks that were significantly enhanced only at a fluence of 80 J/cm^2, and (*3*) peaks that were dose dependently increased at 40 and 80 J/cm^2. The mean values were logarithmically (base 2) rescaled for better visualization of the big differences in absolute values; heat maps (color scheme 30 exponential) were generated with the EP:Clust software (http://www.bioinf.ebc.ee/EP/EP/EPCLUST/) (36).

RESULTS

The most abundant di- or polyunsaturated PCs in humans and laboratory animals such as mice are molecular species containing linoleic or arachidonic acid in combination with palmytic or stearic acid. Based on previously identified and functionally characterized types of OxPCs, we calculated *m/z* values of oxidation products of these four PCs encompassing major types of oxidized residues (i.e., fragmented ω-terminal, fragmented α,β-unsaturated, fragmented terminal furan-containing, nonfragmented linear (hydro(pero)xides, keto) and nonfragmented prostane ring-containing species) (Supplementary Table III). In addition, several fragmented species generated by oxidation of PCs containing docosahexaenoic acid were selected. The HPLC-MS/MS analysis of phosphocholine-containing lipids was performed in positive ion mode by SRM at 99 precursor *m/z* values (Supplementary Table III) using a specific PC product ion (*m/z* 184) corresponding to the cleaved phosphocholine residue. The use of SRM instead of scheduled (i.e., retention-time dependent) SRM, as being applied in our earlier work on a small and defined analyte set (34), was chosen to realize a nontargeted screening for compounds having *m/z* 184 as a common fragment but having quite different retention times. Nonenzymatically oxidized PAPC, PLPC, SAPC, and SLPC, each containing a mixture of oxidized PC species (Supplementary Fig. I for OxPAPC and OxPLPC), were analyzed by the same HPLC-ESI-MS/MS procedure to estimate retention time of OxPCs. As expected, due to oxidative fragmentation of fatty acid residue or the addition of oxygen atom(s), OxPCs eluted from the reversed-phase column significantly earlier as compared with their unoxidized precursors and separated well from the bulk of unoxidized PCs (Supplementary Fig. II). Therefore, only molecular species eluting within 8 min (dashed line in Supplementary Fig. II) were analyzed in further experiments.

Analysis of lipid extracts from human skin fibroblasts showed that PC peaks eluting within 8 min were detectable at 97 out of 99 tested *m/z* values. Typically, several peaks eluting at different times were detected at each *m/z* value (Supplementary Table III and **Fig. 1**). We could unequivocally identify four fragmented species for which commercial standards were available, namely POVPC, PGPC, PONPC, and PAzPC. The relative abundances of unidentified isobaric peaks in UVA-irradiated fibroblasts were similar to or higher than peaks with known identity (Fig. 1). Multiple peaks may represent isobaric compounds with different chemical composition or may correspond to multiple positional isomers of the same OxPC, which elute as clusters of poorly separated peaks (e.g., PLPC-OH [*m/z* 774] and PLPC-OOH [*m/z* 790]; Fig. 1). Genuine isobaric compounds most likely represent abnormal oxidized or short-chain polar species of PC as judged by the short retention time in reversed-phase chromatography, which was often disproportional to their high molecular weight and can be explained by the inclusion of oxygen atoms. The patterns of oxidized/polar PCs in fibroblasts and several other tested types of biological samples were well reproducible within and between experiments (see figures below); however, we observed significant variation in the relative abundance of individual peaks in different types of cells and tissues as well as in control versus UVA-irradiated samples (Supplementary Fig. III; Figs. 3, 5, 6 and data not shown). Thus, different biological samples and treatments demonstrate specific "fingerprints" of oxidized/polar PCs that can be characterized by the analytical procedure described in this paper.

To identify PC species that are regulated by oxidative stress, cultured human skin fibroblasts were irradiated with UVA light at 340–400 nm. UVA stimulates the formation of singlet oxygen in dermal fibroblasts (37) followed by activation of enzymes generating reactive oxygen species (38). PLs, and to a lower extent free fatty acids, can (presumably when minimally oxidized) generate singlet oxygen under UVA exposure (39). The UVA irradiation had minimal effects on the levels of unoxidized PCs (**Fig. 2**) but stimulated accumulation of fragmented OxPCs in a fluence-dependent manner (**Fig. 3**). Irradiation of cells for the same time (20 min) at a half of radiance resulted in significantly lower accumulation of OxPCs (data not shown). Thus, at least within the time frame of the experiment, fluence is the major factor determining the magnitude of elevation of OxPCs as compared with the time of irradiation.

To test whether our HPLC-ESI-MS/MS procedure can quantify absolute concentrations of OxPCs, signal calibration was performed using commercial standards of POVPC, PGPC, PONPC, and PAzPC (Supplementary Table II). Assuming the volume of a human dermal foreskin fibroblast cell to be 3.5 pL and a cell density of 500,000 cells on 9.6 cm^2, cellular levels of fragmented OxPCs achieved upon irradiation at 80 J/cm^2 were calculated to be 19.37 ± 0.24 μM (POVPC), 0.33 ± 0.03 μM (PGPC), 4.14 ± 0.13 μM (PONPC), and 0.89 ± 0.05 μM (PAzPC). If we assume that similar amounts of fragmented species were generated from SAPC, which is present in cells at similar amounts as PAPC, then the combined concentration of several fragmented PCs reaches the low micromolar range, which is about 10-fold higher than in unirradiated cells. It is known that micromolar concentrations of exogenously added fragmented OxPCs are toxic to cells (40–42); the effect is likely to be stronger for cell-associated OxPCs. Thus, quantitative data allow hypothesizing that fragmented OxPCs can play a role as mediators of UVA-induced cell death.

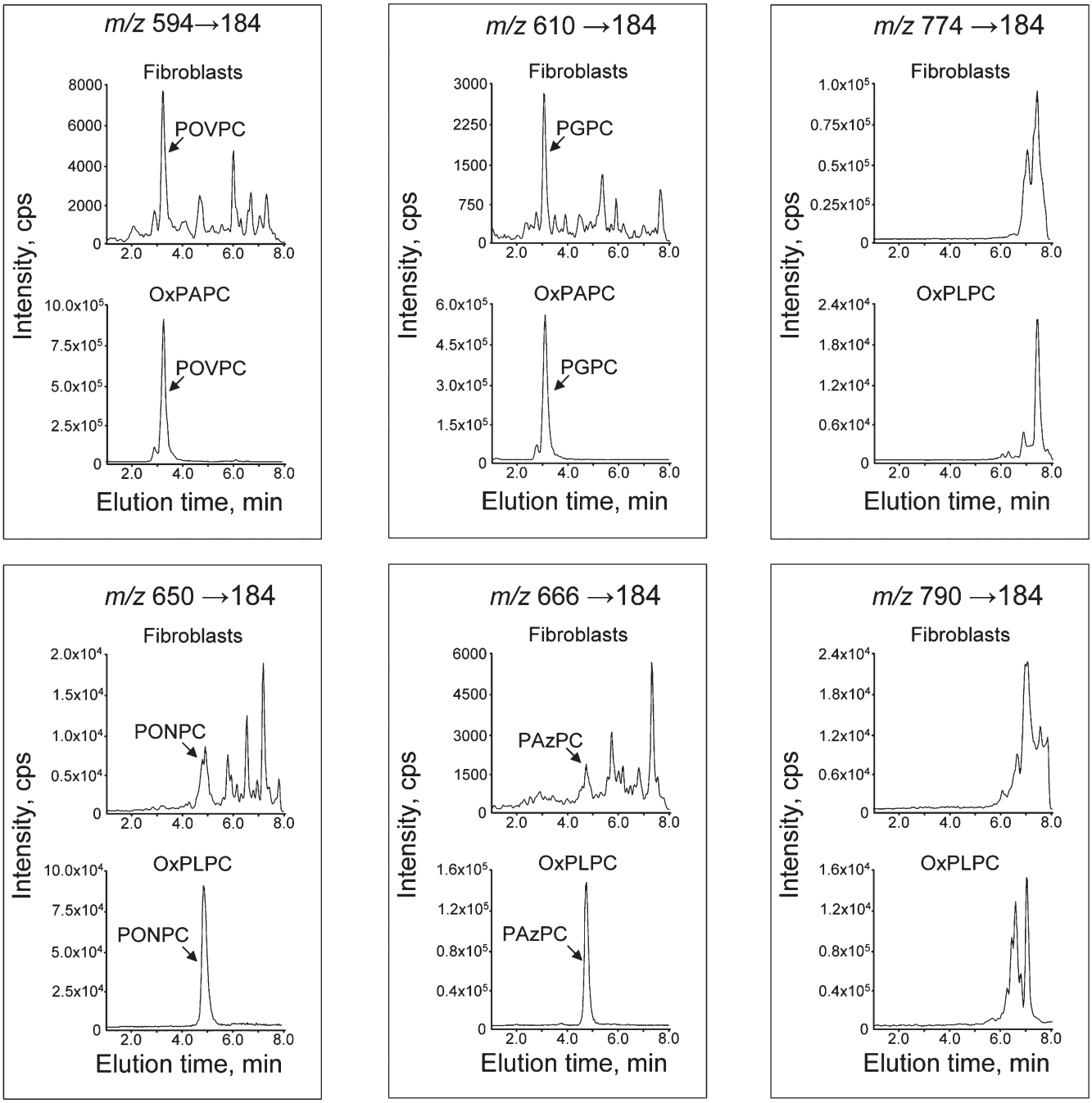

Fig. 1. Examples of isobaric PCs at *m/z* values corresponding to fragmented (594, 610, 650, 666) or full-length (774, 790) OxPC species. The upper chromatograms show the presence in fibroblasts of multiple isobaric peaks. The full-length (nonfragmented) species elute as clusters of closely migrating peaks, which can result from the presence of positional isomers that are poorly separated due to identical chemical composition. The arrows point to the peaks identified using commercially available synthetic standards for POVPC, PGPC, PONPC, and PAzPC. The lower chromatograms show monitoring of the same *m/z* values within crude mixtures of OxPCs generated by nonenzymatic oxidation of corresponding precursors. The presence in OxPAPC and OxPLPC of single peaks coeluting with synthetic standards confirms the specificity of mass spectrometry detection. The total abundance of unidentified isobaric peaks in fibroblasts is comparable or exceeds that of peaks with known identity.

To determine whether the method can be applied for fingerprinting of a wide spectrum of oxidized and polar PCs including peaks with unknown identity, two fluences of UVA were selected, where the lower fluence of 40 J/cm^2 would reach the surface of the skin during 112 min of sun exposure around noon at northern latitude of 35° (e.g., Memphis, Tennessee or Nicosia, Cyprus), of which 30% would penetrate to the dermal compartment (43). This physiological fluence is within the range used for UVA-1 phototherapy and does not induce considerable apoptosis in cultured fibroblasts, as shown by cell morphology 16 h after irradiation (**Fig. 4 A–C**), immunoblotting for PARP cleavage (44) (Fig. 4 D), and staining for active caspase 3 (10). The higher pathological fluence (80 J/cm^2) used

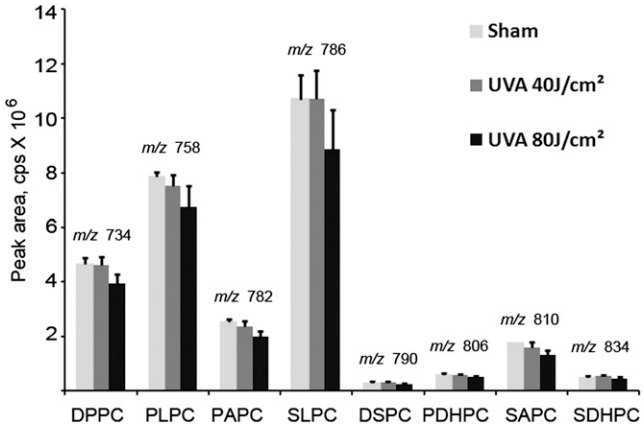

Fig. 2. Short-term UVA irradiation has minimal effect on the levels of unoxidized PCs. Human dermal fibroblasts were irradiated for 10 (40 J/cm^2) or 20 (80 J/cm^2) min. The incubation was stopped by immediate washing and the addition of acidic methanol. Lipid extract from cells grown on two 35 mm wells (1/1,200th) was injected for analysis of unoxidized species. The elution/detection was performed within 15 min. The relative amounts of unoxidized PCs were determined by the Analyst 1.5 software as areas of peaks identified using commercially available standards. There was a trend for decreased levels of PLs at the 80 J/cm^2 fluence; however, the differences were not statistically significant. Error bars indicate standard deviations of analytical triplicates (corresponding to six biological replicates).

in this study led to massive apoptosis of dermal fibroblasts 16 h after exposure as shown by PARP cleavage and changed the morphology of cells stained with crystal violet (Fig. 4). The cumulated amount of OxPLs with known cytotoxic effects at 80 J/cm^2 may contribute to UVA-induced cell death. UVA fluence-dependently up-regulated 217 polar PC species out of ~500 that were reproducibly detected in all or in the majority of samples; a further 242 polar species were significantly up-regulated only at the higher fluence of 80 J/cm^2 (**Fig. 5**). In some cases, irradiation up-regulated several peaks of certain *m/z* values, whereas other peaks of the same *m/z* value were regulated minimally if at all (Fig. 6). The differential effects of oxidative stress may help to distinguish unoxidized isobaric peaks from molecular species regulated by oxidation. Furthermore, the data in **Fig. 6** illustrate that our fingerprinting technique can be used to select OxPCs that are the most informative biomarkers for a specific type of biological samples and oxidative stress.

Our procedure detected multiple peaks of unknown identity that were up-regulated upon UVA irradiation. An advantage of the HPLC procedure that was used in this study is compatibility with mass spectrometry detection in the negative mode, which allows characterization of oxidized and unoxidized acyl residues in PCs (45–47). As a proof of principle, we identified endogenous fragmented OxPCs, such as POVPC, PGPC, PONPC, and PAzPC, using LC-ESI-MS/MS in negative mode using MS/MS parameters as described in Nakanishi et al. (48) (Supplementary Fig. IV). Correct identification of these molecular species was additionally confirmed by spiking samples with commercial standards (data not shown). Thus, the method can help in structural characterization of unidentified oxidized/polar PCs.

DISCUSSION

The major goal of this work was to develop a method for detection of a broad spectrum of OxPCs within one analytical run. Our approach introduced several modifications to the existing procedures for mass spectrometry of OxPCs, which together resulted in a faster procedure sufficiently sensitive for the detection of OxPLs in different biological samples.

An important step in our method is sample preparation by two LLE steps (i.e., acidic methanol/hexane extraction and Folch phase separation). This procedure is simple, inexpensive, and efficiently removes compounds with polarity significantly higher or significantly lower than OxPCs, and especially neutral lipids, which otherwise strongly contaminate the detector, resulting in considerable deterioration of the signal after multiple injections of real samples. In our experience, consequent analyses of more than 40 samples purified by LLE did not produce a detectable decrease in signal intensity of internal standards or endogenous lipids (data not shown). As compared with the procedure based on solid-phase extraction that was used in our previous work (34), the LLE method has significantly higher throughput when performed manually. An additional advantage of this method is that incubation of cells in culture dishes can be instantly terminated by the addition of acidic methanol, which, in contrast to the Folch solvent mixture, does not dissolve plastic. Thus, we avoid a common procedure of scraping cells into saline that can introduce artifacts due to enzymatic degradation of OxPLs and artificial oxidation.

Another improvement of existing methods that was introduced by us recently (34) is the application of core-shell chromatographic material resulting in fast and efficient separation of multiple molecular species. Hundreds of oxidized/polar PCs were analyzed in just 8 min; a 15-min run separated unoxidized PCs in addition to OxPLs. Thus, our method is significantly faster than procedures described previously (e.g., 50 min [24]; > 40 min [49]), thus resulting in significantly lower instrument time and corresponding costs, which are the major factors limiting the use of mass spectrometry for routine analysis.

Sensitivity is an important issue in the analysis of trace analytes in biological samples that are available in limited amounts (e.g., cultured cells or samples from small laboratory animals, such as murine vessels and bronchoalveolar lavage fluid). Our method has sufficient sensitivity to be used in experimental applications of this sort. A wide variety of oxidized/polar PCs encompassing different structural classes was detected in lipid extract obtained from fibroblasts grown on a cell culture vessel surface of 1.6 cm^2. The low amount of cells needed for one analysis makes realistic comprehensive experiments analyzing detailed time- and dose kinetics in multiple replicates. On the other hand, higher amounts of lipid extracts can be injected

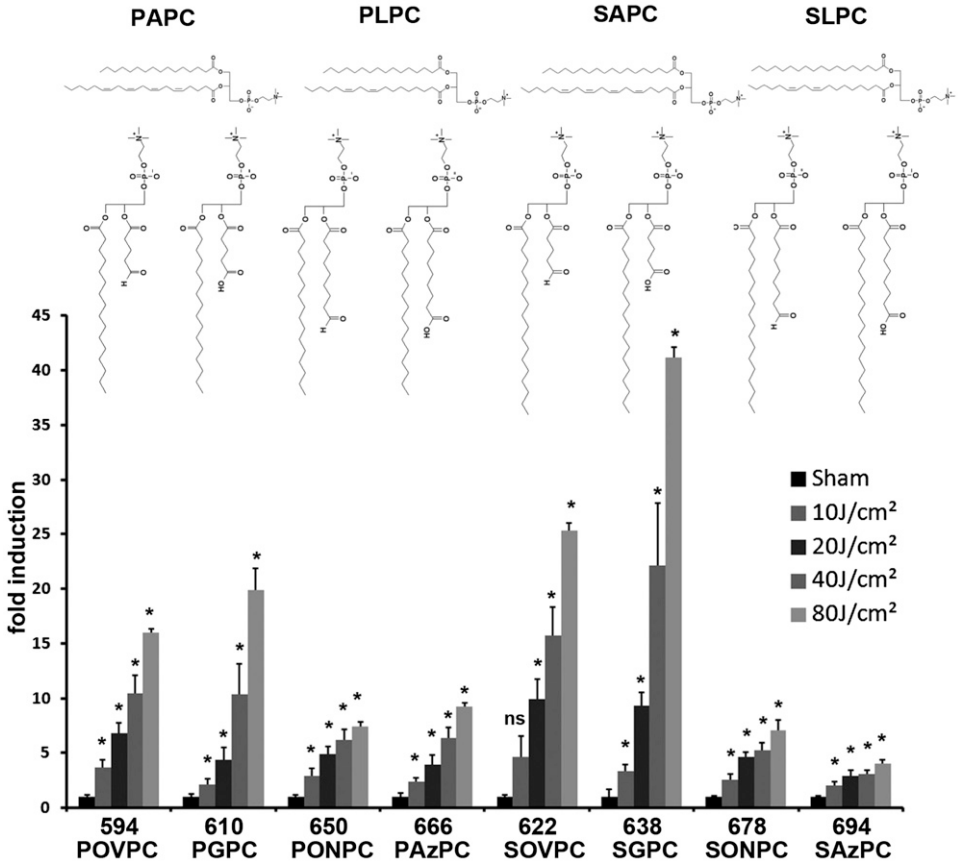

Fig. 3. Fluence-dependence of accumulation of fragmented OxPCs. Human dermal fibroblasts were irradiated for 2.5 (10 J/cm^2), 5 (20 J/cm^2), 10 (40 J/cm^2), or 20 (80 J/cm^2) min. The incubation was stopped by immediate washing and addition of acidic methanol. One twelfth of the lipid extract from irradiated human dermal fibroblasts grown on two 35 mm wells was injected for analysis of oxidized species. OxPCs produced from PAPC and PLPC were identified using commercial standards. Products of SAPC and SLPC were tentatively identified based on their *m/z* values, presence in OxSAPC or OxSLPC, and characteristic shift in retention time as compared with homologs containing palmitoyl residues. Error bars indicate standard deviations of analytical triplicates (corresponding to six biological replicates).

when improved detection of minor species of OxPCs is required. Although the method is intended for fingerprinting experiments based on relative quantification of oxidized/polar PCs in control and treated groups, we demonstrated here that the procedure can be used for absolute quantification of those molecular species for which commercial standards are available.

Application of this method to investigate the PC oxidation repertoire in dermal fibroblasts under oxidative stress induced by UVA irradiation confirmed our previous findings that specific, biologically active OxPCs (e.g., *m/z* 828) are dose dependently increased by this treatment (10). In addition, we observed accumulation of a plethora of nonfragmented and fragmented OxPCs. This opens the possibility to identify novel OxPLs that may have detrimental effects in photoageing and UV-induced pathologies as well as photoproducts that mediate beneficial effects of UVA radiation, which is used for therapy of inflammatory skin diseases. This task, which was outside of the scope of this work, can be pursued using other modes of HPLC-MS/MS (47, 48, 50), high-resolution mass spectrometry (51), group-specific reagents (27, 31), and other approaches known in the field. Due to the large number of molecular species being detected and the lack of standards for many putative OxPCs, it was impossible to unequivocally identify the majority of peaks. However, as a proof of principle, we

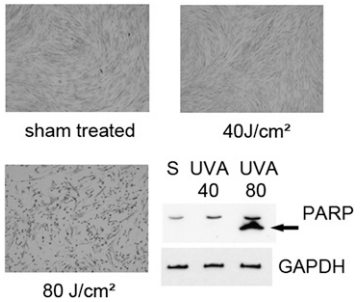

Fig. 4. Effects of UVA irradiation on morphology and apoptosis of human dermal fibroblasts 16 h after irradiation. A–C: Crystal violet staining of human dermal fibroblasts 16 h after UVA irradiation. D: Western blotting shows PARP cleavage indicative of apoptosis in cells irradiated at 80 J/cm^2 only. The lower panel shows staining for GAPDH protein. Lipids were extracted immediately after the end of irradiation, but these data show long-term effects of UVA.

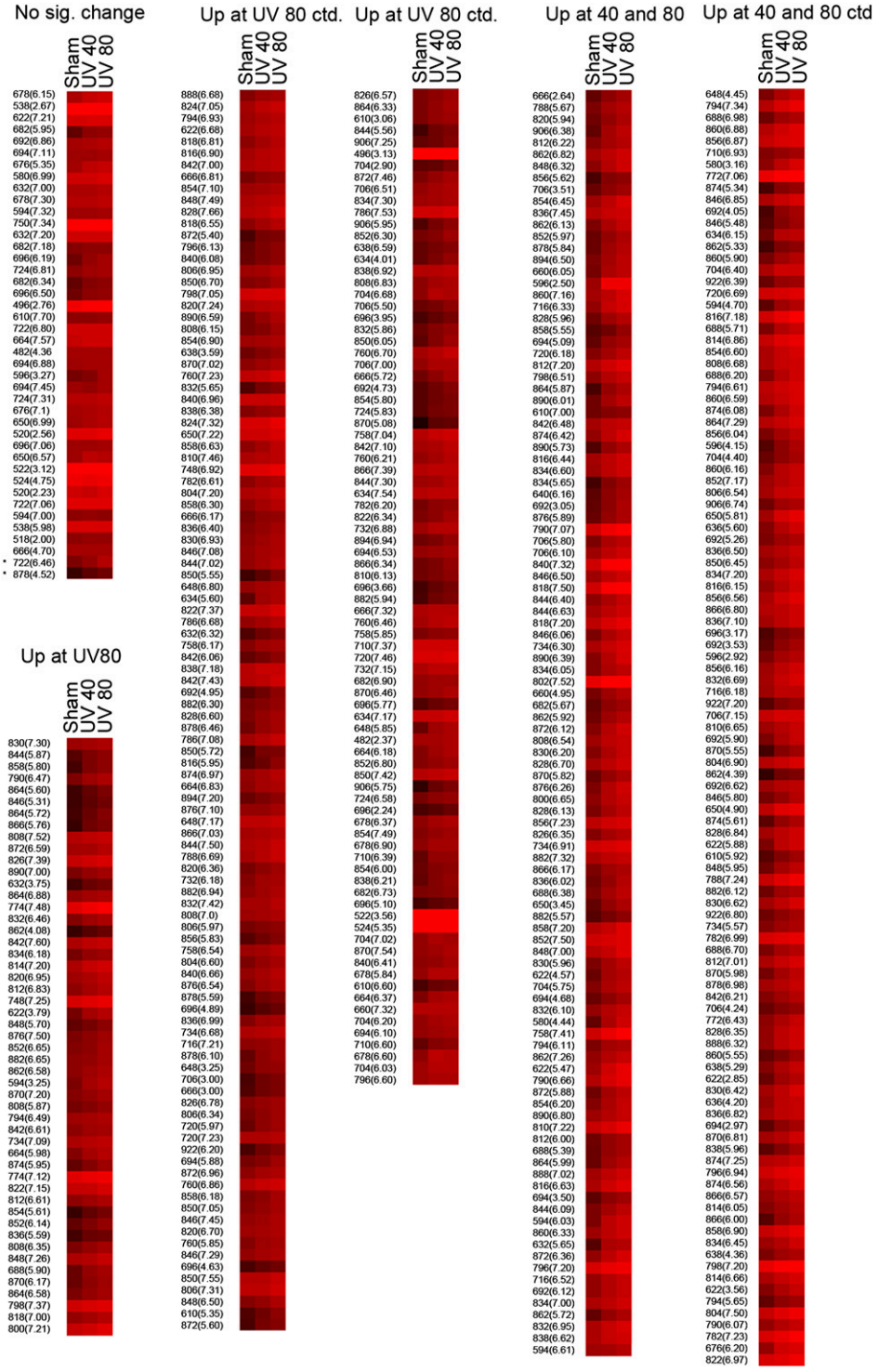

Fig. 5. Heat map representing color-coded abundance levels of OxPCs. One twelfth of the lipid extract from irradiated human dermal fibroblasts grown on two 35 mm wells was injected for analysis of oxidized species. The procedure was performed in triplicate (corresponding to six biological replicates) for each condition. Peaks eluting within 8 min were recorded, and then the eluate was switched to waste. The map is an output from EPCLUST software (color scheme "30 exponential") and presents mean values from analytical triplicates (corresponding to six biological replicates) of sham, UVA 40, and 80 J/cm^2 irradiated dermal fibroblasts. Values were logarithmically rescaled for better visualization of a high dynamic range. The peaks are grouped into nonregulated (40 peaks, "No sig. change"), significantly increased only at 80 J/cm^2 (242 peaks, "Up at 80"), and significantly increased by UVA 40 J/cm^2 and further increased by UVA 80 J/cm^2 (217 peaks, "Up at 40 and 80"). Asterisks mark two peaks significantly increased by UVA 40 J/cm^2 but not by 80 J/cm^2 and thus added to the nonregulated group. For each group, peaks are listed starting with the highest significance of increase of UVA 40 J/cm^2 treated versus sham treated. Significance was determined by *t*-test and subsequent adjustment with the Benjamini-Hochberg method to a false discovery rate of 0.05.

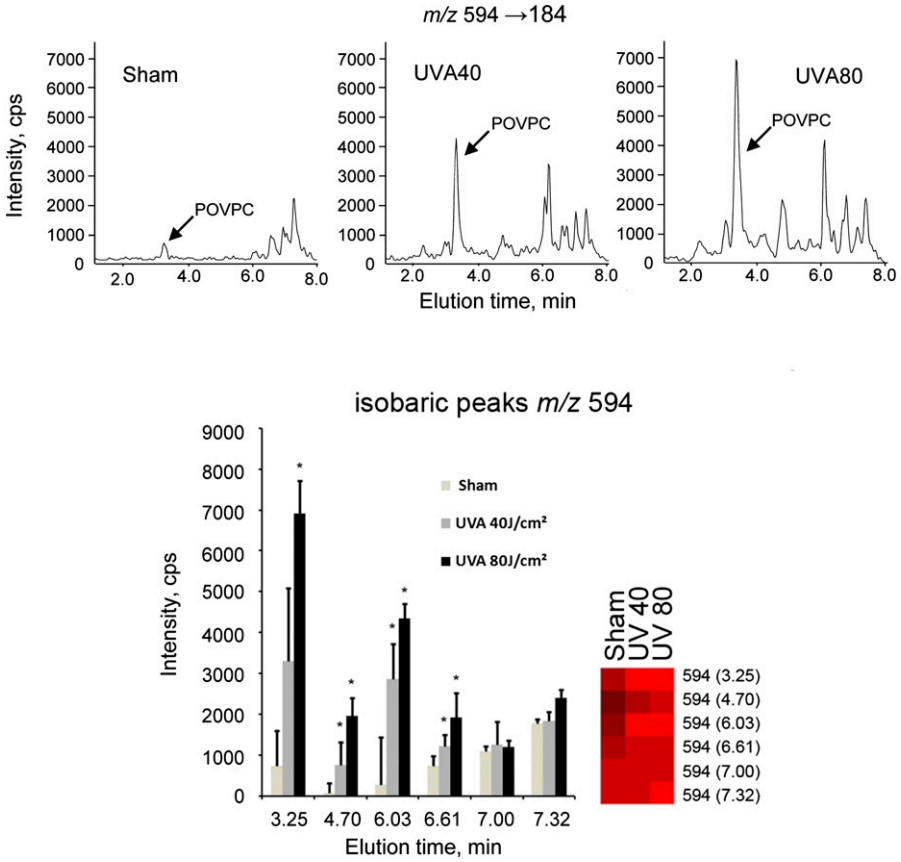

Fig. 6. Differential regulation of isobaric peaks by UVA-irradiation. The data show that at certain *m/z* values (represented by *m/z* 594 in this Figure) only a proportion of peaks were up-regulated by UVA-irradiation, while other peaks were not significantly changed. Representative chromatographic profiles (upper panel) or mean values presented as bar graph or heat map (lower panel). Error bars indicate standard deviations of analytical triplicates (corresponding to six biological replicates). Asterisks indicate significant increase of UVA irradiated as compared with sham-treated cells (*t*-test, Benjamini-Hochberg adjusted to false discovery rate of 0.05).

demonstrated here identification by MS/MS fragmentation studies in the negative ion mode of four molecular species of endogenously formed OxPCs accumulating in UVA-irradiated fibroblasts.

At several *m/z* values for which standards were available, unidentified isobaric peaks were equally or more abundant than known species of the same *m/z*. Oxidized and short-chain unoxidized PLs have high polarity and therefore can influence the structure and functions of biological membranes. Therefore, the "dark matter" of oxidized/polar PCs detected by our method is likely to be relevant to cellular (patho)physiology and deserves more detailed study and characterization of individual molecular species.

In summary, we describe a procedure for analysis of a broad spectrum of PCs up-regulated by UVA irradiation. This procedure is intended to be used as a first step in the characterization of oxidized/polar species of OxPCs induced by different types of oxidative stress and disease. Advantages of this fingerprinting procedure include a simple and robust process of sample precleaning, short instrument time, and high sensitivity sufficient for many biological applications.

The authors thank Jarmila Uhrinova for technical assistance.

REFERENCES

1. Bochkov, V. N., O. V. Oskolkova, K. G. Birukov, A. L. Levonen, C. J. Binder, and J. Stockl. 2010. Generation and biological activities of oxidized phospholipids. *Antioxid. Redox Signal.* **12:** 1009–1059.
2. Tsimikas, S., and Y. I. Miller. 2011. Oxidative modification of lipoproteins: mechanisms, role in inflammation and potential clinical applications in cardiovascular disease. *Curr. Pharm. Des.* **17:** 27–37.
3. Fraley, A. E., G. G. Schwartz, A. G. Olsson, S. Kinlay, M. Szarek, N. Rifai, P. Libby, P. Ganz, J. L. Witztum, and S. Tsimikas. 2009. Relationship of oxidized phospholipids and biomarkers of oxidized low-density lipoprotein with cardiovascular risk factors, inflammatory biomarkers, and effect of statin therapy in patients with acute coronary syndromes: results from the MIRACL (Myocardial Ischemia Reduction With Aggressive Cholesterol Lowering) trial. *J. Am. Coll. Cardiol.* **53:** 2186–2196.
4. Wittwer, J., and M. Hersberger. 2007. The two faces of the 15-lipoxygenase in atherosclerosis. *Prostaglandins Leukot. Essent. Fatty Acids.* **77:** 67–77.
5. Clark, S. R., C. J. Guy, M. J. Scurr, P. R. Taylor, A. P. Kift-Morgan, V. J. Hammond, C. P. Thomas, B. Coles, G. W. Roberts, M. Eberl, et al. 2011. Esterified eicosanoids are acutely generated by 5-lipoxygenase in primary human neutrophils and in human and murine infection. *Blood.* **117:** 2033–2043.
6. Morgan, L. T., C. P. Thomas, H. Kuhn, and V. B. O'Donnell. 2010. Thrombin-activated human platelets acutely generate oxidized

docosahexaenoic-acid-containing phospholipids via 12-lipoxygenase. *Biochem. J.* **431:** 141–148.
7. Savaskan, N. E., C. Ufer, H. Kuhn, and A. Borchert. 2007. Molecular biology of glutathione peroxidase 4: from genomic structure to developmental expression and neural function. *Biol. Chem.* **388:** 1007–1017.
8. Fisher, A. B. 2011. Peroxiredoxin 6: a bifunctional enzyme with glutathione peroxidase and phospholipase A activities. *Antioxid. Redox Signal.* **15:** 831–844.
9. Birukov, K. G., V. N. Bochkov, A. A. Birukova, K. Kawkitinarong, A. Rios, A. Leitner, A. D. Verin, G. M. Bokoch, N. Leitinger, and J. G. Garcia. 2004. Epoxycyclopentenone-containing oxidized phospholipids restore endothelial barrier function via Cdc42 and Rac. *Circ. Res.* **95:** 892–901.
10. Gruber, F., O. Oskolkova, A. Leitner, M. Mildner, V. Mlitz, B. Lengauer, A. Kadl, P. Mrass, G. Kronke, B. R. Binder, et al. 2007. Photooxidation generates biologically active phospholipids that induce heme oxygenase-1 in skin cells. *J. Biol. Chem.* **282:** 16934–16941.
11. Gruber, F., H. Mayer, B. Lengauer, V. Mlitz, J. M. Sanders, A. Kadl, M. Bilban, R. de Martin, O. Wagner, T. W. Kensler, et al. 2010. NF-E2-related factor 2 regulates the stress response to UVA-1-oxidized phospholipids in skin cells. *FASEB J.* **24:** 39–48.
12. Peres, P. S., V. A. Terra, F. A. Guarnier, R. Cecchini, and A. L. Cecchini. 2011. Photoaging and chronological aging profile: Understanding oxidation of the skin. *J. Photochem. Photobiol. B.* **103:** 93–97.
13. Tanaka, N., S. Tajima, A. Ishibashi, K. Uchida, and T. Shigematsu. 2001. Immunohistochemical detection of lipid peroxidation products, protein-bound acrolein and 4-hydroxynonenal protein adducts, in actinic elastosis of photodamaged skin. *Arch. Dermatol. Res.* **293:** 363–367.
14. Domingues, M. R., A. Reis, and P. Domingues. 2008. Mass spectrometry analysis of oxidized phospholipids. *Chem. Phys. Lipids.* **156:** 1–12.
15. Tyurina, Y. Y., V. A. Tyurin, A. M. Kaynar, V. I. Kapralova, K. Wasserloos, J. Li, M. Mosher, L. Wright, P. Wipf, S. Watkins, et al. 2010. Oxidative lipidomics of hyperoxic acute lung injury: mass spectrometric characterization of cardiolipin and phosphatidylserine peroxidation. *Am. J. Physiol. Lung Cell. Mol. Physiol.* **299:** L73–L85.
16. Tyurina, Y. Y., V. A. Tyurin, V. I. Kapralova, K. Wasserloos, M. Mosher, M. W. Epperly, J. S. Greenberger, B. R. Pitt, and V. E. Kagan. 2011. Oxidative lipidomics of gamma-radiation-induced lung injury: mass spectrometric characterization of cardiolipin and phosphatidylserine peroxidation. *Radiat. Res.* **175:** 610–621.
17. Maciel, E., P. Domingues, and M. R. Domingues. 2011. Liquid chromatography/tandem mass spectrometry analysis of long-chain oxidation products of cardiolipin induced by the hydroxyl radical. *Rapid Commun. Mass Spectrom.* **25:** 316–326.
18. Greenberg, M. E., M. Sun, R. Zhang, M. Febbraio, R. Silverstein, and S. L. Hazen. 2006. Oxidized phosphatidylserine-CD36 interactions play an essential role in macrophage-dependent phagocytosis of apoptotic cells. *J. Exp. Med.* **203:** 2613–2625.
19. Maskrey, B. H., A. Bermudez-Fajardo, A. H. Morgan, E. Stewart-Jones, V. Dioszeghy, G. W. Taylor, P. R. Baker, B. Coles, M. J. Coffey, H. Kuhn, et al. 2007. Activated platelets and monocytes generate four hydroxyphosphatidylethanolamines via lipoxygenase. *J. Biol. Chem.* **282:** 20151–20163.
20. Wynalda, K. M., and R. C. Murphy. 2010. Low-concentration ozone reacts with plasmalogen glycerophosphoethanolamine lipids in lung surfactant. *Chem. Res. Toxicol.* **23:** 108–117.
21. Thomas, C. P., L. T. Morgan, B. H. Maskrey, R. C. Murphy, H. Kuhn, S. L. Hazen, A. H. Goodall, H. A. Hamali, P. W. Collins, and V. B. O'Donnell. 2010. Phospholipid-esterified eicosanoids are generated in agonist-activated human platelets and enhance tissue factor-dependent thrombin generation. *J. Biol. Chem.* **285:** 6891–6903.
22. Domingues, M. R., C. Simoes, J. P.da Costa, A. Reis, and P. Domingues. 2009. Identification of 1-palmitoyl-2-linoleoyl-phosphatidylethanolamine modifications under oxidative stress conditions by LC-MS/MS. *Biomed. Chromatogr.* **23:** 588–601.
23. O'Donnell, V. B. 2011. Mass spectrometry analysis of oxidized phosphatidylcholine and phosphatidylethanolamine. *Biochim. Biophys. Acta.* **1811:** 818–826.
24. Morgan, A. H., V. J. Hammond, L. Morgan, C. P. Thomas, K. A. Tallman, Y. R. Garcia-Diaz, C. McGuigan, M. Serpi, N. A. Porter, R. C. Murphy, et al. 2010. Quantitative assays for esterified oxylipins generated by immune cells. *Nat. Protoc.* **5:** 1919–1931.
25. Spickett, C. M., I. Wiswedel, W. Siems, K. Zarkovic, and N. Zarkovic. 2010. Advances in methods for the determination of biologically relevant lipid peroxidation products. *Free Radic. Res.* **44:** 1172–1202.
26. Morgan, A. H., V. Dioszeghy, B. H. Maskrey, C. P. Thomas, S. R. Clark, S. A. Mathie, C. M. Lloyd, H. Kuhn, N. Topley, B. C. Coles, et al. 2009. Phosphatidylethanolamine-esterified eicosanoids in the mouse: tissue localization and inflammation-dependent formation in Th-2 disease. *J. Biol. Chem.* **284:** 21185–21191.
27. Watson, A. D., N. Leitinger, M. Navab, K. F. Faull, S. Horkko, J. L. Witztum, W. Palinski, D. Schwenke, R. G. Salomon, W. Sha, et al. 1997. Structural identification by mass spectrometry of oxidized phospholipids in minimally oxidized low density lipoprotein that induce monocyte/endothelial interactions and evidence for their presence in vivo. *J. Biol. Chem.* **272:** 13597–13607.
28. Podrez, E. A., E. Poliakov, Z. Shen, R. Zhang, Y. Deng, M. Sun, P. J. Finton, L. Shan, M. Febbraio, D. P. Hajjar, et al. 2002. A novel family of atherogenic oxidized phospholipids promotes macrophage foam cell formation via the scavenger receptor CD36 and is enriched in atherosclerotic lesions. *J. Biol. Chem.* **277:** 38517–38523.
29. Podrez, E. A., T. V. Byzova, M. Febbraio, R. G. Salomon, Y. Ma, M. Valiyaveettil, E. Poliakov, M. Sun, P. J. Finton, B. R. Curtis, et al. 2007. Platelet CD36 links hyperlipidemia, oxidant stress and a prothrombotic phenotype. *Nat. Med.* **13:** 1086–1095.
30. Gao, S., R. Zhang, M. E. Greenberg, M. Sun, X. Chen, B. S. Levison, R. G. Salomon, and S. L. Hazen. 2006. Phospholipid hydroxyalkenals, a subset of recently discovered endogenous CD36 ligands, spontaneously generate novel furan-containing phospholipids lacking CD36 binding activity in vivo. *J. Biol. Chem.* **281:** 31298–31308.
31. Subbanagounder, G., J. W. Wong, H. Lee, K. F. Faull, E. Miller, J. L. Witztum, and J. A. Berliner. 2002. Epoxyisoprostane and epoxycyclopentenone phospholipids regulate monocyte chemotactic protein-1 and interleukin-8 synthesis. Formation of these oxidized phospholipids in response to interleukin-1beta. *J. Biol. Chem.* **277:** 7271–7281.
32. Broekhuyse, R. M. 1968. Phospholipids in tissues of the eye. I. Isolation, characterization and quantitative analysis by two-dimensional thin-layer chromatography of diacyl and vinyl-ether phospholipids. *Biochim. Biophys. Acta.* **152:** 307–315.
33. Rendl, M., J. Ban, P. Mrass, C. Mayer, B. Lengauer, L. Eckhart, W. Declerq, and E. Tschachler. 2002. Caspase-14 expression by epidermal keratinocytes is regulated by retinoids in a differentiation-associated manner. *J. Invest. Dermatol.* **119:** 1150–1155.
34. Oskolkova, O. V., T. Afonyushkin, B. Preinerstorfer, W. Bicker, E. von Schlieffen E, E. Hainzl, S. Demyanets, G. Schabbauer, W. Lindner, A. D. Tselepis, J. Wojta, B. R. Binder, and V. N. Bochkov. 2010. Oxidized phospholipids are more potent antagonists of lipopolysaccharide than inducers of inflammation. *J. Immunol.* **185:** 7706–7712.
35. Benamini, Y., and Y. Hochberg. 1995. Controlling the false discovery rate: a practical and powerful approach to multiple testing. *J. R. Statist. Soc. B.* **57:** 289–300.
36. Brazma, A., and J. Vilo. 2000. Gene expression data analysis. *FEBS Lett.* **480:** 17–24.
37. Vile, G. F., S. Basu-Modak, C. Waltner, and R. M. Tyrrell. 1994. Heme oxygenase 1 mediates an adaptive response to oxidative stress in human skin fibroblasts. *Proc. Natl. Acad. Sci. USA.* **91:** 2607–2610.
38. Valencia, A., and I. E. Kochevar. 2008. Nox1-based NADPH oxidase is the major source of UVA-induced reactive oxygen species in human keratinocytes. *J. Invest. Dermatol.* **128:** 214–222.
39. Baier, J., T. Maisch, J. Regensburger, C. Pollmann, and W. Baumler. 2008. Optical detection of singlet oxygen produced by fatty acids and phospholipids under ultraviolet A irradiation. *J. Biomed. Opt.* **13:** 044029.
40. Chen, R., L. Yang, and T. M. McIntyre. 2007. Cytotoxic phospholipid oxidation products. Cell death from mitochondrial damage and the intrinsic caspase cascade. *J. Biol. Chem.* **282:** 24842–24850.
41. Fruhwirth, G. O., A. Moumtzi, A. Loidl, E. Ingolic, and A. Hermetter. 2006. The oxidized phospholipids POVPC and PGPC inhibit growth and induce apoptosis in vascular smooth muscle cells. *Biochim. Biophys. Acta.* **1761:** 1060–1069.
42. Qin, J., F. D. Testai, S. Dawson, J. Kilkus, and G. Dawson. 2009. Oxidized phosphatidylcholine formation and action in oligodendrocytes. *J. Neurochem.* **110:** 1388–1399.
43. Mang, R., and J. Krutmann. 2005. UVA-1 phototherapy. *Photodermatol. Photoimmunol. Photomed.* **21:** 103–108.

44. Oliver, F. J., G. de la Rubia, V. Rolli, M. C. Ruiz-Ruiz, de Murcia G, and J. M. Murcia. 1998. Importance of poly(ADP-ribose) polymerase and its cleavage in apoptosis. Lesson from an uncleavable mutant. *J. Biol. Chem.* **273:** 33533–33539.
45. Nakanishi, H., Y. Iida, T. Shimizu, and R. Taguchi. 2010. Separation and quantification of sn-1 and sn-2 fatty acid positional isomers in phosphatidylcholine by RPLC-ESIMS/MS. *J. Biochem.* **147:** 245–256.
46. Pulfer, M., and R. C. Murphy. 2003. Electrospray mass spectrometry of phospholipids. *Mass Spectrom. Rev.* **22:** 332–364.
47. Yin, H., B. E. Cox, W. Liu, N. A. Porter, J. D. Morrow, and G. L. Milne. 2009. Identification of intact oxidation products of glycerophospholipids in vitro and in vivo using negative ion electrospray iontrap mass spectrometry. *J. Mass Spectrom.* **44:** 672–680.
48. Nakanishi, H., Y. Iida, T. Shimizu, and R. Taguchi. 2009. Analysis of oxidized phosphatidylcholines as markers for oxidative stress, using multiple reaction monitoring with theoretically expanded data sets with reversed-phase liquid chromatography/tandem mass spectrometry. *J. Chromatogr. B Analyt. Technol. Biomed. Life Sci.* **877:** 1366–1374.
49. Sun, M., S. C. Finnemann, M. Febbraio, L. Shan, S. P. Annangudi, E. A. Podrez, G. Hoppe, R. Darrow, D. T. Organisciak, R. G. Salomon, et al. 2006. Light-induced oxidation of photoreceptor outer segment phospholipids generates ligands for CD36-mediated phagocytosis by retinal pigment epithelium: a potential mechanism for modulating outer segment phagocytosis under oxidant stress conditions. *J. Biol. Chem.* **281:** 4222–4230.
50. Reis, A., M. R. Domingues, F. M. Amado, A. J. Ferrer-Correia, and P. Domingues. 2007. Radical peroxidation of palmitoyl-lineloyl-glycerophosphocholine liposomes: identification of long-chain oxidised products by liquid chromatography-tandem mass spectrometry. *J. Chromatogr. B Analyt. Technol. Biomed. Life Sci.* **855:** 186–199.
51. Davis, B., G. Koster, L. J. Douet, M. Scigelova, G. Woffendin, J. M. Ward, A. Smith, J. Humphries, K. G. Burnand, C. H. Macphee, et al. 2008. Electrospray ionization mass spectrometry identifies substrates and products of lipoprotein-associated phospholipase A2 in oxidized human low density lipoprotein. *J. Biol. Chem.* **283:** 6428–6437.